

## Stark Field Control of Nonadiabatic Dynamics in Triatomic Hydrogen

Frank Baumgartner and Hanspeter Helm

*Department of Physics, University of Freiburg, Stefan-Meier-Strasse 19, D-79104 Freiburg, Germany*  
(Received 18 December 2009; published 11 March 2010)

We show experimentally that an external electric field can be used to control the amplitudes of nonadiabatic paths taken by a dissociating molecule. In the example presented here, this control is achieved by Stark-field mixing in  $H_3$  Rydberg states with different decay paths. The final state continuum is in each path formed by three-particle wave packets of slow neutral hydrogen atoms in their electronic ground state. Their momentum vector correlations show signs of interference, since the molecule can access the *identical* continuum via two distinctly different paths, involving different nonadiabatic coupling mechanisms. As an added feature a preferred alignment of the fragmentation plane in the laboratory frame emerges, corresponding to a selective dissociation of molecules oriented along the field direction.

DOI: 10.1103/PhysRevLett.104.103002

PACS numbers: 33.57.+c, 82.37.Np

Many fundamental aspects of molecular physics such as molecule formation and dissociation arise from nonadiabatic couplings between the electronic and nuclear motion. Direct access to the dependence of these couplings on molecular coordinates has largely eluded experimental observation to date, except for diatomics where dynamics reduces to a single vectorial distance corresponding to radial and rotational couplings [1]. In polyatomic systems the larger number of degrees of freedom complicates the observation and description of dynamical properties [2]. During the last decade powerful experimental techniques have been brought to bear on nonadiabatic processes: Ultrafast lasers make it possible to follow the course of a chemical reaction [3–5], molecular beam technology allows the quantum state preparation of reactants as well as the state selective detection of products [6–8], and novel multidimensional coincidence measurements provide hitherto inaccessible information about vector correlations in molecular dynamics [9–12].

Neutral triatomic hydrogen, the simplest example of a polyatomic molecule, frequently serves as a prototypical system for investigating molecular dynamics beyond the limits of the Born-Oppenheimer approximation [10,13–18]. Even for a simple molecule like  $H_3$  the quantitative information inherent in the vector correlation maps poses difficult challenges to theory. It was not until recently, that Galster, Lepetit, and Jungen succeeded in predicting the principal structures observed in a Dalitz plot by the use of semiclassical trajectory models [19–21].

Here we add a new feature of experimental control in this context. We show that the Stark effect can be used to control the amplitudes of nonadiabatic paths taken by a dissociating molecule. In the example presented here, an  $H_3$  molecule in the metastable  $2p^2A_2''$  state (abbreviated  $2p$ ) is coupled to the short-lived  $2s^2A_1'$  level (abbreviated  $2s$ ), building up a superposition of quasidiscrete electronic states

$$|\Psi\rangle = \alpha|2s\rangle + \beta|2p\rangle. \quad (1)$$

In the absence of an external electric field both unperturbed states predissociate into the repulsive ground-state surface. A molecule in the superposition state (1) can therefore access the three-particle dissociation continuum via two distinct paths (see Fig. 1), involving different nonadiabatic coupling operators  $V_{2s}$  and  $V_{2p}$ . The magnitude of the external electric field determines the amplitudes  $\alpha$  and  $\beta$ . Describing the rovibrational part of the wave function with  $|\chi\rangle$ , we may formally view the dissociation process in a time-dependent approach as a sequence of two steps:

During a first period the quasibound molecular state accesses the repulsive ground-state surface at a time  $t_1$ , forming a superposition of two continuum wave packets at molecular distances. The wave function

$$\begin{aligned} |\Psi^m\rangle_{(t_1)} &= \alpha V_{2s}|2s\rangle|\chi\rangle + \beta V_{2p}|2p\rangle|\chi\rangle \\ &= \alpha|\phi_s\rangle + \beta|\phi_p\rangle \end{aligned} \quad (2)$$

is building up under the action of the nonadiabatic coupling

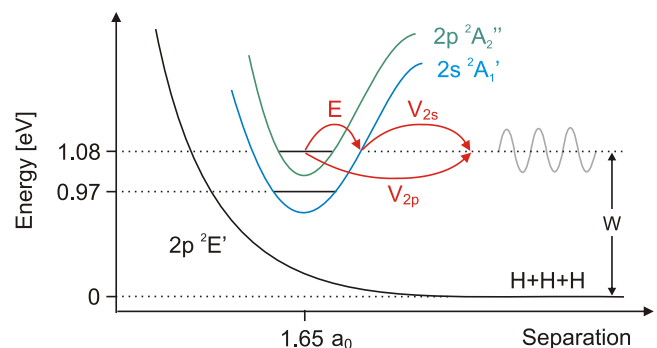


FIG. 1 (color online). Schematic predissociation channels for the  $2p^2A_2''$  state in an external electric field. The strength of the nonadiabatic couplings,  $V_{2s}$  and  $V_{2p}$ , to the repulsive ground-state surface are greatly different. The action of the electric field is indicated by the arrow marked  $E$ .

operators  $V$ . This period is followed by an evolution of the wave packets  $|\phi_s\rangle$  and  $|\phi_p\rangle$  on the ground-state potential energy surface [22], resulting in a continuum wave function

$$|\Psi^c\rangle_{(t)} = \int_{t_1}^t e^{iHt'} (\alpha|\phi_s\rangle + \beta|\phi_p\rangle) dt' \quad (3)$$

with the Hamiltonian  $H$  describing the motion of the three hydrogen atoms on the dissociative  $2pE'$  ground-state surface. In the limit  $t \rightarrow \infty$  (at the position sensitive detector) the wave function (3) is mapped onto the product wave function of three separated hydrogen atoms

$$|\Psi^c\rangle = \phi_1(\vec{k}_1)\phi_2(\vec{k}_2)\phi_3(\vec{k}_3), \quad (4)$$

the  $\vec{k}_i$  being the center-of-mass momenta of the free hydrogen atoms. The space of  $\vec{k}$  vectors is restricted by energy and momentum conservation. In our experiment we determine, for one molecule at a time,  $\vec{k}_1$ ,  $\vec{k}_2$ , and  $\vec{k}_3$ . The result for many such measurements provides us with a map of the probability distribution  $||\Psi^c||^2$ . Phase differences that were accumulated on the two paths in Eq. (3) will show up as interference effects in this map.

In this sense our experiment amounts to a double-slit experiment involving two wave packets of three correlated, slow hydrogen atoms in their ground electronic state. Their interference pattern is projected into the correlation map of the three atomic momentum vectors.

Our experiment is performed with a fast-beam apparatus, discussed previously [12,16,23], but now modified by a Stark-field section as shown schematically in Fig. 2. The neutral  $H_3$  molecules are produced in near-resonant charge transfer of 3 keV  $H_3^+$  ions in a cesium vapor cell. At its exit residual ions are deflected by a small electric field. The charge-exchange process initially generates a wide spectrum of neutral states, nearly all of which dissociate within a few ns. Only molecules in the rotationless  $2p^2A_2'$  ( $N=0, K=0$ ) state are metastable [24]. Because of their long lifetime  $\approx 700$  ns [25], only these molecules can transit to the Stark-field section, which is situated 30 cm downstream from the charge-transfer cell. Two half-cylindrical electrodes with a radius of 1 cm, positioned 3 mm apart at the closest point, establish the Stark field. During their  $\approx 50$  ns transit time through the Stark-field region the molecules experience an inhomogeneous dc field, whose maximum strength can be varied between 0 and 20 kV/cm.

The undissociated fraction of the neutral molecules is intercepted by a beam flag at a distance of 10 cm from the

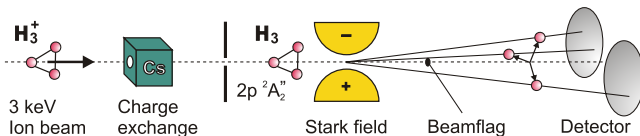


FIG. 2 (color online). Overview of the experimental setup.

Stark-field region. Fragments from predissociation with sufficient transverse momentum pass the flag and reach the multihit coincidence detector after a free flight of 239 cm. The arrival times and positions of the three hydrogen atoms are registered by the detector [9]. Our new detection electronics [26] achieve a spatial resolution of 80  $\mu\text{m}$  and a temporal resolution of 50 ps.

Owing to the slow radiative transition from the metastable state [27] to the short-lived  $2s^2A_1'$  level, dissociation of the field-free  $2s^2A_1'$  and  $2p^2A_2''$  levels can be investigated separately. This is possible because the kinetic energy release  $W$  of the two states differs by 100 meV, easily discernible in our experiment. Examples of Dalitz maps for the two states, recorded in the field-free case, are shown in Fig. 3 for the lowest vibrational level of the  $2p^2A_2''$  and  $2s^2A_1'$  states. The position of an event inside the circular Dalitz plot [28] reflects the relative orientation of the momentum vectors of the three hydrogen atoms in the center-of-mass frame, as indicated in Fig. 3 on the left. The map reflects the internal molecular couplings that initiate the dissociation process and that are experienced by the 3 H atoms as they evolve from molecular distances to the separated atom limit. The conventional Dalitz coordinates

$$x = \frac{1}{\sqrt{3}}(\varepsilon_2 - \varepsilon_1) \quad \text{and} \quad y = \varepsilon_3 - \frac{1}{3} \quad (5)$$

relate the kinetic energy of the  $i$ th atom in the center-of-mass frame,  $\varepsilon_i = |\vec{k}_i|^2/(2mW)$ , with the orientation of the three momentum vectors  $\vec{k}_i$  ( $i = 1, 2, 3$ ). The quantities  $\varepsilon_i$  are normalized to the total kinetic energy  $W$  released in the dissociation process,  $W = \sum_i \varepsilon_i$ . The magnitude of  $W$  is determined for each molecule and serves to identify the initial state involved in dissociation. Here we focus on metastable molecules in the vibrational ground state,  $\nu_0$ . Molecules in higher vibrational levels are present in the beam as well. Their summed abundance amounts to  $<20\%$ . Their energy release is distinctly different and they do not contribute to the signals discussed here.

The  $2s$  state accesses the continuum via vibrational coupling, the  $2p$  state on the other hand can do so in second

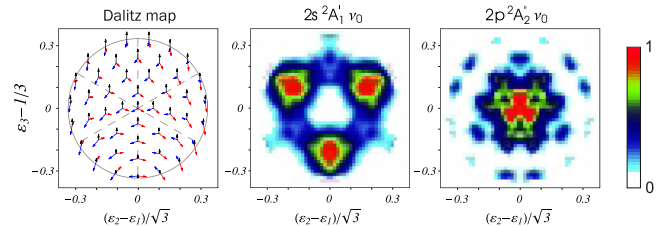


FIG. 3 (color online). Dalitz maps of the lowest rotational levels of the vibrationless  $2s^2A_1'$  and  $2p^2A_2''$  states obtained in the absence of an external electric field. The diagram on the left illustrates the momentum vector alignment corresponding to specific positions in the Dalitz map. A definition of the energy scales is given in Eq. (5) above.

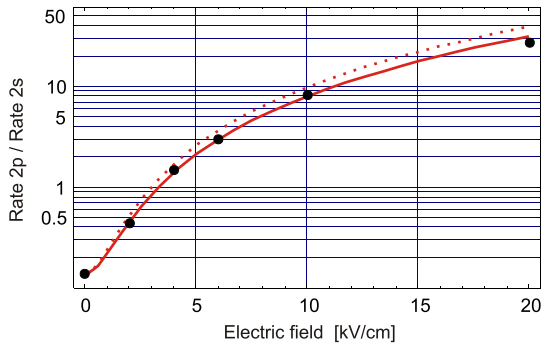


FIG. 4 (color online). The observed ratio of three-body dissociation rates of the metastable  $2p^2A_2''$  state and the  $2s^2A_1'$  state for different electric fields is shown by the full circles. The dotted line gives the prediction from a Stark model based on purely hydrogenic wave functions. The solid curve results when the transition-dipole moment of Petsalakis *et al.* [30] is used.

order only, via rotational coupling [29]. Hence the two states exhibit completely different correlation patterns: While the Dalitz plot of the  $2p$  level is dominated by near-equilateral momentum vector arrangements, the  $2s$  state preferably dissociates into obtuse isosceles configurations largely avoiding the symmetric momentum arrangement. Theory has recently forwarded explicit predictions for the origin of the pattern observed for the  $2s$  state [19–21].

The predominant effect of Stark mixing is the decay of the metastable molecule by indirect coupling to the ground-state continuum via the admixed  $2s$  character. The natural lifetimes of the two excited states  $\tau_{2s} = 200$  fs and  $\tau_{2p} = 700$  ns differ by 6 orders of magnitude. Therefore the experiment weights the state admixture  $\alpha$  with an amplification factor  $\sqrt{700 \text{ ns}/200 \text{ fs}} = 1870$ . As a result, even weak admixtures of  $2s$  character significantly shorten the lifetime of the metastable  $2p$  level. For the field range used in the experiment the fraction of the admixed  $2s$  wave function is always very small, amounting to no more than 0.26% at 20 kV/cm.

In Fig. 4 we compare the observed three-body decay rate of the  $2p^2A_2''$  level with the prediction from a perturbation-theory based Stark model using the  $2s$ - $2p$  coupling matrix element of Petsalakis *et al.* [30]. Note that the dissociation rate of the  $2s^2A_1'$  level is practically unaffected by the  $2p$  admixture, but serves as a convenient experimental calibration of the ratio of rates at zero electric field. As a result of the Stark mixing the momentum correlations observed for the  $2p$  state undergo dramatic changes. The strong influence of the external electric field on the predissociation is apparent from the vector correlation maps for the vibrationless  $2p^2A_2''$  state at different electric-field strengths shown in Fig. 5.

For a molecule initially in the  $2p$  state the branching between the  $2p$  and  $2s$  paths is predicted to be about equal at 4 kV/cm. At 20 kV/cm the branching amounts to 96% along the  $2s$  path with only 4% remaining on the

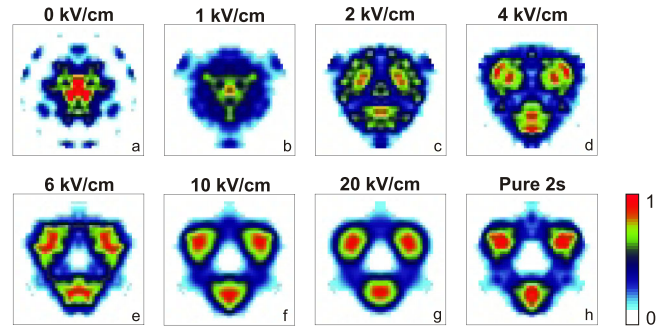


FIG. 5 (color online). Influence of an external electric field on the observed momentum vector correlations of the vibrationless  $2p^2A_2''$  level. The axis labeling is identical to that shown in Fig. 3 but omitted here for clarity of presentation. Color scale is as given in Fig. 3.

parent  $2p$  channel. Hence practically the full  $2s$  correlation pattern builds up in the Dalitz map of the Stark  $2p$  state at 20 kV/cm. This is apparent from a comparison of Fig. 5(g) with Fig. 5(h). The latter shows the field-free result for the  $2s$  state.

Interference features develop in the intermediate field range ( $E = 2$ – $4$  kV/cm), where the amplitudes of both excited states are similar. These interference patterns in the Dalitz plot of the  $2p$  state cannot be explained in terms of a simple addition of the two field-free maps. Rather their interpretation calls for a superposition treatment outlined in the introduction above.

The direction of the Stark field, parallel to the detector and perpendicular to the molecular beam axis, was chosen to ensure an optimum sensitivity with regard to changes in the orientation of dissociated molecules. Our measurements show that the effect of angular-momentum mixing is reflected in a laboratory alignment of the fragmentation plane. For reasons of momentum conservation this plane lies perpendicular to the molecular main symmetry axis, its normal vector representing the spatial orientation of the  $2p_z$  orbital at the time of dissociation. In the field-free case one would expect an isotropic distribution of the fragmentation plane, whereas the presence of the Stark field should lead to preferred dissociation of  $H_3$  molecules aligned along the field direction.

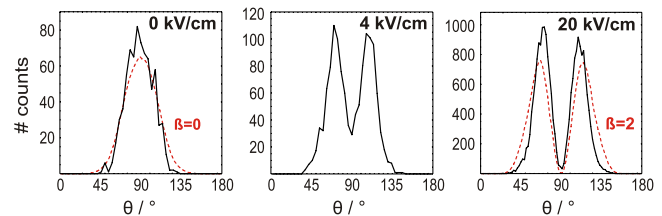


FIG. 6 (color online). Spatial distribution of the main symmetry axis for  $2p^2A_2''$  molecules predissociated in the Stark field. The results at 0 and 20 kV/cm are compared to a Monte Carlo simulation given by the dashed curves. The orientation of the molecular symmetry axis in the external electric field is clearly apparent.

Our experimental results in Fig. 6 display this effect very clearly, with  $\theta$  defining the angle between the electric field and the molecule's main symmetry axis in the laboratory frame. An alignment parameter  $\beta = 0$  corresponds to the isotropic case, whereas  $\beta = 2$  describes a  $\cos^2\theta$  distribution oriented along the electric-field axis. In order to enable a direct comparison we evaluated these two limiting distributions by means of a Monte Carlo simulation (accounting for the experimental detection efficiency) and depicted them as the dashed lines in Fig. 6. At  $E = 0$  kV/cm our experimental observation is in good agreement with the model of an isotropic distribution of the fragmentation plane. As the electric field rises the distribution begins to develop a growing dip around  $\theta = 90^\circ$ , until it resembles the  $\beta = 2$  model at  $E = 20$  kV/cm. This documents that the degree of Stark mixing is anisotropic and most pronounced for  $H_3$  molecules whose  $p_z$  orbital is oriented along the electric-field axis.

Our measurements give a very clear demonstration of the effect of angular-momentum mixing on the vector correlation maps and the spatial orientation of the fragmentation plane: As the field strength rises, an increasing alignment of dissociated  $2p$  molecules along the field axis is observed, while at the same time the Dalitz plot proceeds from the typical  $2p^2A_2''$  features to the distinctly different  $2s^2A_1'$  features. In the transition region around  $E = 4$  kV/cm an interference pattern appears in the correlation map of the Stark  $2p$  state. It results from the fact that the dissociating molecule can be described as a superposition of three-particle wave packets which coherently access the *same* continuum via two different channels, each case experiencing a different nonadiabatic transition and a different evolution on the ground-state potential energy surface. By adjusting the electric-field strength we are able to fine-tune the amplitudes of the two interfering paths, which offers the opportunity to experimentally control the magnitude of nonadiabatic coupling.

Unlike studies of pure decay rates, our kinematically complete experiment records the dissociation dynamics in terms of the center-of-mass momentum vectors *and* the molecular orientation in laboratory space. At this point it is awaiting a thorough theoretical discussion on the motion of three-particle wave packets on the ground-state energy surfaces of  $H_3$ . The recent achievements [19–21] in the theoretical description of predissociation of the  $2s^2A_1'$  state promise that a similar treatment of the  $2p^2A_2''$  state will, once it is available, enable a detailed analysis of our data. We expect that a quantitative understanding of the observed interference effects will greatly improve our knowledge in the field of nonadiabatic couplings.

We kindly thank Professor J.S. Briggs and Dr. U. Galster for helpful discussions and M. Gisi for the develop-

ment of the new detection electronics. This research was supported by the DFG Grant HE 2525/5.

- 
- [1] H. Lefebvre-Brion and R. Field, *The Spectra and Dynamics of Diatomic Molecules* (Elsevier, New York, 2004).
  - [2] D. Yarkony, *J. Chem. Phys.* **100**, 18 612 (1996).
  - [3] J. Sage *et al.*, *Phys. Rev. Lett.* **86**, 4966 (2001).
  - [4] S. Trushin *et al.*, *Chem. Phys. Lett.* **376**, 282 (2003).
  - [5] A. Stolov *et al.*, *Int. Rev. Phys. Chem.* **22**, 377 (2003).
  - [6] A. Sanov *et al.*, *J. Chem. Phys.* **111**, 664 (1999).
  - [7] K. Liu, *Annu. Rev. Phys. Chem.* **52**, 139 (2001).
  - [8] M. Bradke and R. Loomis, *J. Chem. Phys.* **118**, 7233 (2003).
  - [9] U. Müller, T. Eckert, M. Braun, and H. Helm, *Phys. Rev. Lett.* **83**, 2718 (1999).
  - [10] D. Strasser, L. Lammich, H. Kreckel, S. Krohn, M. Lange, A. Naaman, D. Schwalm, A. Wolf, and D. Zafman, *Phys. Rev. A* **66**, 032719 (2002).
  - [11] C.M. Laperle, J.E. Mann, T.G. Clements, and R.E. Continetti, *Phys. Rev. Lett.* **93**, 153202 (2004).
  - [12] U. Galster, F. Baumgartner, U. Müller, H. Helm, and M. Jungen, *Phys. Rev. A* **72**, 062506 (2005).
  - [13] W. Ketterle, H.-P. Messmer, and H. Walther, *Europhys. Lett.* **8**, 333 (1989).
  - [14] C. Bordas and H. Helm, *Phys. Rev. A* **45**, 387 (1992).
  - [15] V. Kokoouline and C.H. Greene, *Phys. Rev. A* **68**, 012703 (2003).
  - [16] U. Galster, U. Müller, and H. Helm, *Phys. Rev. Lett.* **92**, 073002 (2004).
  - [17] J.C. Tully, *Faraday Discuss.* **127**, 463 (2004).
  - [18] J. Mann, C. Laperle, J. Savee, and R. Continetti, *Chem. Phys. Lett.* **473**, 34 (2009).
  - [19] U. Galster, *Phys. Rev. A* (to be published).
  - [20] B. Lepetit, R. Abrol, and A. Kuppermann, *Phys. Rev. A* **76**, 040702(R) (2007).
  - [21] M. Lehner and M. Jungen, *J. Phys. B* **42**, 065101 (2009).
  - [22] J. Krause, K. Kulander, J. Light, and A. Orel, *J. Chem. Phys.* **96**, 4283 (1992).
  - [23] I. Mistrík, R. Reichle, H. Helm, and U. Müller, *Phys. Rev. A* **63**, 042711 (2001).
  - [24] G. Gellene and R. Porter, *J. Chem. Phys.* **79**, 5975 (1983).
  - [25] C. Bordas, P. Cosby, and H. Helm, *J. Chem. Phys.* **93**, 6303 (1990).
  - [26] M. Gisi, Master's thesis, Fakultät für Physik, Universität Freiburg, 2007.
  - [27] Z. Peng, A. Kuppermann, and J. Wright, *Chem. Phys. Lett.* **175**, 242 (1990).
  - [28] R. Dalitz, *Philos. Mag.* **44**, 1068 (1953).
  - [29] I. Dabrowski and G. Herzberg, *Can. J. Phys.* **58**, 1238 (1980).
  - [30] I. Petsalakis, G. Theodorakopoulos, and J. Wright, *J. Chem. Phys.* **89**, 6850 (1988).